UNITED STATES DEPARTMENT OF THE INTERIOR

GEOLOGICAL SURVEY

Structural and heat-flow implications of infrared anomalies at Mt. Hood, Oregon

by

Jules D. Friedman

U.S. Geological Survey, Denver, Colorado 80225

and

David Frank

U.S. Geological Survey, Seattle, Washington

Open-File Report 77-599

1977

Structural and heat-flow implications of infrared anomalies at Mt. Hood, Oregon

by

Jules D. Friedman

U.S. Geological Survey, Denver, Colorado 80225

David Frank

U.S. Geological Survey, Seattle, Washington

Abstract

Surface thermal features occur in an area of 9700 m^2 at Mt. Hood, on the basis of an aerial line-scan survey made April 26, 1973. The distribution of the thermal areas below the summit of Mt. Hood, shown on planimetrically corrected maps at 1:12,000, suggests structural control by a fracture system and brecciated zone peripheral to a hornblende-dacite plug dome (Crater Rock), and by a concentric fracture system that may have been associated with development of the present crater. The extent and inferred temperature of the thermal areas permits a preliminary estimate of a heat discharge of 10 megawatts, by analogy with similar fumarole and thermal fields of Mt. Baker, Washington. This figure includes a heat loss of 4 megawatts (MW) via conduction, diffusion, evaporation, and radiation to the atmosphere, and a somewhat less certain loss of 6 MW via fumarolic mass transfer of vapor and advective heat loss from runoff and ice melt. The first part of the estimate is based on two-point models for differential radiant exitance and differential flux via conduction, diffusion, evaporation, and

radiation from heat balance of the ground surface. Alternate methods for estimating volcanogenic geothermal flux that assume a quasi-steady state heat flow also yield estimates in the 5-11 MW range. Heat loss equivalent to cooling of the dacite plug dome is judged to be insufficient to account for the heat flux at the fumarole fields.

Contents

List of illustrations

Introduction

Aerial infrared surveys of the Cascade Range volcanoes were undertaken between 1970 and 1973 by the U.S. Geological Survey to record the location and extent of geothermally warm ground and fumarole fields in the Cascade Range (Friedman and Frank, 1973).

This report gives data from two aerial surveys: April 19, 1972 and April 26, 1973, flown over Mt. Hood, Oregon, by the U.S. Forest Service expressly for the U.S. Geological Survey. The aerial scanner used in this survey was an RS-7 line-scan system equipped with a detector sensitive to infrared radiation in the 8-14 μm band.

Geology of Mt. Hood

Mt. Hood, Oregon, whose summit location (fig. 1) is approximately $45^{\circ}22'N$, $121^{\circ}42'W$, is a relatively symmetrical andesitic to dacitic composite volcano rising to an altitude of 3392 m and occupying 242 km^2. The height of the volcanic edifice above the surrounding terrain is about 1800 m.

Mt. Hood volcano was built during late Pleistocene time in the area of two late Pliocene volcanic centers that erupted sequences of olivine basalt, olivine andesite, and pyroxene andesite. The present cone is composed of approximately 193 km^3 of olivine-, pyroxene-, and hornblende-dacite lavas and pyroclastic debris (Wise, 1969, p. 969, 993). The main cone was built before the Fraser Glaciation (Late Wisconsin), but a plug dome was extruded below the summit about 1700 years ago; another plug dome was extruded at the same location perhaps as

recently as 220±150 years ago, based on radiocarbon dating of pyroclastic flow deposits derived from that dome (Crandell and Rubin, 1977, p. 406).

Geology of Crater Rock area

The upper part of the youngest plug dome forms Crater Rock which is situated within the crater 450 m south of the summit between 3170 and 3220 m altitude. Analyses 138 and 141 reported by Wise (1969, p. 999, Table 16), of samples taken from Crater Rock (Wise, oral commun., 1977) contain 14.4 and 16.8 percent normative quartz, respectively, and both analyses indicate a little more than 62 percent SiO_2. The composition of one, and very likely both, plug domes, (map unit Q_{hh} of Wise, 1968, p. 82-83) is thus dacite, and is similar to dacite domes at other Cascade Range volcanoes (e.g., Mt. St. Helens summit dome, Lassen Peak, Chaos Crags, and Bumpass Mountain). Destruction of the south rim of the present crater probably preceded the extrusion of the 1700-year old plug domes by a substantial length of time (Crandell, D. R., 1977, oral commun.).[1]

[1] At St. Augustine volcano, Alaska, a similar dacitic plug dome was extruded between February 6 and 15, 1976, after the explosive eruption of January 22-23, 1976 had reopened the vent, breached, and explosively cleared the lava dome of 1964 (Kienle and Forbes, 1976, p. 41; and David Johnston, oral commun., 1977). The only thermal precursor to the eruptions was an increase in the temperature of a fumarole located on the contact between the 1935 and 1964 lava domes. The new crater was opened along this boundary (Kienle and Forbes, 1976, p. 36).

Associated with the hornblende-dacite plug dome (Q_{hh}) is a brecciated zone that may extend beneath thermally-altered clay immediately north of Crater Rock. This crush zone may extend for a greater distance around Crater Rock than presently mapped.

Elsewhere in the Crater Rock area and especially in the vicinity of Steel Cliff, another Holocene map unit (Q_{hp}) designates pyroclastic deposits interbedded with flows; this unit includes altered pyroclastic debris possibly older than the Crater Rock plug dome (Wise, 1968). Because highly altered material overlies both Q_{hp} and Q_{hh}, the exact position of the contact between these two units is not known (Wise, 1977, oral comm.).

Historical eruptive activity

Macdonald (1972, p. 441) lists one period of unverified historical eruptive activity at Mt. Hood, ca. 1801. Whether this reported eruption corresponds to a late phase of extrusion of the dacite plug dome is not known. Interestingly, Sapper (1927, p. 343, in German), states that according to Perrey (1865), Mt. Hood was "active many times" (mehrfach tätig) in 1854, in 1859 when illuminated vapor clouds (erleuchtete dampfmassen) were seen, and 1865 (1859 and 1865 were also mentioned by Ayres and Crosswell, 1951, p. 35). Sapper also reports a distended white vapor (?) column (rauchsäulen) on August 28, 1907. The present writers have not seen the original reports upon which Sapper based his statements, several of which may have been newspaper accounts. Sylvester (1908) reported indications of increasing fumarolic activity

in 1908 at and near Crater Rock, in the main crater on the south side of Mt. Hood. In view of the present fumarolic emission from Mt. Hood, and of bursts of fumarolic emission accompanied by large vapor columns from other Cascade volcanoes (e.g., Mt. Baker in 1975), perhaps the best conclusion to draw from Sapper's reports is that at least spasmodic vapor emission has occurred from Mt. Hood's fumarole fields for more than 100 years.

Fumaroles at Mt. Hood

The fumaroles at Mt. Hood are located at Crater Rock, on the steep east wall (Steel Cliff) of the crater and on the floor of the crater, north and east of Crater Rock (Figures 2, 3, 4). Phillips and Collins (1935, p. 19-20) investigated the temperature regime of four fumaroles in these areas in 1935. Their Fumarole A was a group of small vents 38 m southwest of the old Crater Rock shelter (which is no longer at that site), in an area of hydrothermally-altered warm ground about 10 m in diameter and covered with yellow, white, and greenish sublimates. Vent temperatures on September 8, 1935 averaged 89.4°C (Phillips and Collins, 1935, p. 20). Fumarole B was a large, open vertical vent on the north ridge of Crater Rock (corrected altitude based on current maps is about 3230 m) whose vapor temperature was 71.1°C (Phillips, 1936, p. 45). Fumarole C was an open, vertical vent south of Fumarole B. The temperature 1.2 m below the surface was 48.9°C on September 8, 1935 (Phillips and Collins, 1935, p. 20). Fumarole D, a large and active vent 123 m northeast of the old Crater Rock shelter at the base

of Steel Cliff was recorded at 89.4°C on October 6, 1935 (Phillips, 1936, p. 45). Exactly the same temperature (89.4°C) was recorded at Fumaroles A and D in 1951 (Ayres and Cresswell, 1951, p. 40). For comparative purposes, maximum temperatures recently recorded at selected fumarole fields of the Cascade Range are given in Table 1.

The locations of visible fumarolic emanations as mapped by Wise between 1962 and 1965 are shown by x's on Figure 3.

Infrared anomalies and structural control of thermal areas

The two aerial infrared surveys flown over Mt. Hood in 1972 (Fig. 2) and 1973 recorded thermal emission from the main fumarole field (A, fig. 2) which is part of the hornblende-dacite plug dome, and from the fumarole field in the Devil's Kitchen and Steel Cliff area (B, fig. 2) partly in pyroclastic deposits interbedded with flows.

The fumarole fields appear on the infrared image of April 26, 1973 as a vaguely circular pattern of anomaly clusters in the brecciated zone peripheral to the Crater Rock plug dome, and as a concentric pattern around the open south margin of the main crater. The anomalies are between 3020 m and 3230 m in altitude and in April 1973 covered an area of 9700 m^2 (fig. 4).

An interpretation of this peripheral pattern, consistent with geologic models of fracture systems around vertically prolate magma chambers, is suggested. Such magma chambers that contain intermediate-composition magmas are inferred here to have many structural features in common with dacite plugs. Koide and Bhattacharji (1975, p. 798)

Table 1.--Maximum temperatures recently recorded at selected fumarole fields of the Cascade Range.

Volcanic area	Fumarole field	Site of measurement	Altitude (m)	Boiling point (C)	Recent max. temp. (C)	Date	Reference
Mt. Hood, Oregon	Crater Rock, Steel Cliff	Fumarole vapor	3200	89.4	89.4	1935 1951	Phillips and Collins, 1935; Ayres and Cresswell, 1951
Lassen volcanic region, California	Bumpass Hell	Fumarole vapor	2740	91.0	93.2*	1972	Friedman and Frank, (unpublished data)
		50-cm depth in warm ground			90.0		
Mt. St. Helens, Washington	Southwest slope	50-cm depth in warm ground	2700	91.1	89.0	1973	Friedman and Frank, 1977 b
Mt. Baker, Washington	Dorr	Fumarole vapor	2400	92.1	91.6**	1974 **	Friedman and Frank, 1977 a
		50-cm depth in warm ground			90.0**		
Lassen volcanic region, California	Devil's Kitchen	Fumarole vapor	2030	93.4	100.0	1973	Friedman and Frank, (unpublished data)
		50-cm depth in warm ground			99.4		

* Temperature of nearby fumaroles probably higher

** Before the increased thermal activity of March 10, 1975

found that peripheral radial and en echelon concentric tension fractures develop in plan around vertically elongated magma bodies as a response to stress when magma and hydrothermal-fluid pressure exceeds lithostatic confining pressure. Under these conditions, stress contours (in section) near the apex of magma bodies are almost arcuate, and one of the two maximum shear stress directions would dip toward the extension of the central axis of the magma body (p. 788). Breccia zones may also form along the boundaries of the predominantly concentric and radial fracture zones.

The prolateness of the Crater Rock plug dome is suggested by Wise (1968, p. 98) in his structural sections of Mt. Hood (fig. 6).

We infer that the emplacement and extrusion of the plug dome were controlled or accompanied by the development of a peripheral concentric and radial fracture system and that this fracture system, including the breccia zone around Crater Rock, has controlled the location of the Crater Rock fumarole field, associated warm ground, and infrared anomalies (fig. 2), by providing near-vertical channels along which hydrothermal vapors are convected to the brecciated and altered zones at the surface.[2] Sporadic renewal of this fracture system by hydrothermal or volcanogenic seismic activity may also have occurred (cf historical eruptive activity) during the last 100 years.

[2]

Thermal anomalies similar to those of Mt. Hood have been recorded at dacite domes at Mt. St. Helens, at several dacite domes in the Lassen volcanic region, including Lassen Peak and Bumpass Mountain (unpub. data, 1977), and along margins of dacitic plug domes elsewhere. Many of these anomalies seem to be associated with peripheral structures that developed during or prior to the extrusion of the domes.

Heat budget of thermal areas at Mt. Hood

The geothermal flux Q in the anomalous temperature zones at Mt. Hood is related to the other major components of the heat budget of the ground surface at any time by the following equation:

$$Q = F_b + F_h + F_e + F_{ad}, \qquad (1)$$

where Q is the net geothermal flux, F_b is the differential radiant flux (i.e., F_b approximates the outgoing radiant flux minus the absorbed solar flux minus nondirectional or diffuse sky radiation minus heat flux in the ground as a result of solar radiation), F_h is the outgoing flux of energy from the surface by eddy diffusion and molecular conduction, F_e is the heat flux lost to the atmosphere by evaporation, and F_{ad} is the heat flux carried out of the area advectively by ice melt, stream runoff, and mass transfer to the atmosphere via fumarole and vapor-plume emanations.

Inferred differential radiant exitance from Mt. Hood thermal areas

The differential radiant flux or exitance, F_b, is a measure of the heat exchange with the atmosphere as the result of conductive warming of the earth's surface. The differential radiant exitance from a warm surface in relation to a nearby cold surface can be estimated from a simplified two-point thermal model as expressed below, if adequate data are available on surface temperatures (Birnie, 1973, p. 1-36; and Friedman, Preble, and Jakobsson, 1976, p. 650). The relationship for differential radiant exitance,

$$\int_0^\infty W d\lambda = 5.679 \times 10^{-12} \, (T_0^{\,4} - T_{0'}^{\,4}), \qquad (2)$$

utilizes the Stefan-Boltzmann function for comparing two points on the earth's surface: a warm point T_0 (as mapped by aerial infrared scanner) and an adjacent cold reference point $T_{0'}$, where $Wd\lambda$ is the differential power radiated per unit area, and 5.679×10^{-12} is the Stefan-Boltzmann constant.

Lacking adequate quantitative data on ground temperatures on cold and warm surfaces of the fumarole fields of Mt. Hood, we infer temperatures of the infrared anomalies to fall approximately within the range of those measured by thermistor arrays at similar fumarole fields of the Cascade Range. As a guide, comparison of fumarole temperatures in the Cascade Range (Table 1) in relation to altitude suggests that the Mt. Hood thermal area ranges in temperature (and enthalpy) between that of Mt. St. Helens and the fumarole fields of the Lassen volcanic region. The anomalous thermal areas, as mapped by aerial infrared scanner, are similar in extent of warm ground as well as in maximum fumarole temperatures, to those of Mt. Baker (before 1975).

The differential radiant exitance at the small fumarole fields of Mt. St. Helens was of the order of 80 Wm^{-2} in 1973-4 (Friedman and Frank, 1977b). At the fumarole fields of Mt. Baker, we estimated the differential radiant exitance at 100 Wm^{-2} $\pm$ 15 percent in 1972-1973 (Friedman and Frank, 1977a). After the increase in fumarolic emission in March 1975, the differential radiant exitance increased to about 130 Wm^{-2} (Friedman and Frank, 1977a). The infrared anomalies at Mt. Hood may have a similar range in differential radiant exitance, 80-130 Wm^{-2}, i.e., of the order of 100 Wm^{-2}.

Inferred differential flux via diffusion, conduction, evaporation, and radiation

A significant part of the geothermal flux from volcanogenic or geothermal surface manifestations can be approximated by application of a two-point model for heat balance of the ground surface (Sekioka and Yuhara, 1974). This two-point model considers several mechanisms of heat transfer: differential radiant exitance, heat exchange with the atmosphere via eddy diffusion and molecular conduction, F_h, and evaporation, F_e.

It does not, however, consider heat loss via fumarolic mass transfer and other advective loss, F_{ad}, via warm runoff or ice melt.

The two-point model of Sekioka and Yuhara (1974, p. 2053-2058), as modified by Friedman and Frank (1977a) and adapted for use with calibrated synoptic aerial-infrared-scanner images of Mt. Baker, permits the following simplified relationship,

$$\Delta G = \varepsilon(1 - 0.09m)\ (0.52 + 0.065\ (e_w)^{\frac{1}{2}})\ \sigma\Delta(T_0)^4 + \rho_a c_p D(1 + R)\ \Delta\theta\ , \qquad (3)$$

in which the differential flux via diffusion, conduction, evaporation, and radiation, ΔG (i.e., that flux greater than the heat flux through the cold reference surface) is expressed in terms of integrated emissivity ε ($0.95 \pm .05$) of the surface materials[3], vapor pressure e_w

[3] That the apparent emissivity of surfaces of volcanic rock types approaches unity asymptotically with increased roughening was implied by the work of Gouffe (1945) who showed that the change in apparent emissivity of a surface is a function of cavity shape and integrated emissivity of cavity walls.

(approximately 4.1 mbar at 3000 m altitude), Stefan's constant σ (5.679 x 10^{-12} W cm^{-2}), surface temperature T_0 (^oK) and θ (^oC), as measured at Mount Baker by use of calibrated aerial infrared-scanner images and ground thermistor arrays (Friedman and Frank, 1977a), air density ρ_a (0.909 x 10^{-3} g cm^{-3} at 3000 m altitude), specific heat of air c_p (0.909 x 10^{-3} g cm^{-3}), the transfer velocity D, i.e., the coefficient of external diffusion between the earth's surface and the atmosphere (1.59 cm s^{-1} following Budyko, 1956, p. 46-56), and the Bowen ratio R (Bowen, 1926) equal to 0.3 as determined for Mt. Baker (Friedman and Frank, 1977a) by calculating the ratio of heat loss by eddy diffusion and conduction to heat lost by evaporation by the method of Dawson (1964, p. 155-171).

The combined differential flux ($F_b + F_h + F_e$) was estimated, using this model, as somewhat less than 400 Wm^{-2} at the site B fumarole field, Mt. St. Helens, in 1973. At the Dorr fumarole field and Sherman Crater of Mt. Baker, ($F_b + F_h + F_e$) of the infrared anomalies slightly exceeded 400 Wm^{-2} in 1972-1973. We infer a comparable flux ($F_b + F_h + F_e$) at the infrared anomalies of the Mt. Hood fumarole fields, i.e., of the order of 400 Wm^{-2}. At the high wind speeds characteristic of the summit of Mt. Hood, both F_h and F_e would be somewhat greater.

Inferred heat loss via convection and advection

As yet, no data are available on the F_{ad} component of the heat budget of the Mt. Hood thermal area (Eq. 1). By analogy with Mt. Baker, the Lassen volcanic region, and other thermal areas with active

fumarole fields, F_{ad} is apt to be quantitatively significant. F_{ad} can be divided into two categories at Mt. Baker and Mt. Hood where the thermal area has melted glacier snow and ice and where subglacial fumaroles have created perforation features in the glacier: (1) heat loss to the atmosphere via mass or convective transfer from active fumaroles, and (2) advective heat loss via snow and ice melt and melt-water drainage.

Energy partition estimates at Mt. Baker for the 1972-1973 period suggest that about 30 percent of the total heat discharge of the thermal area is dissipated via each of these mechanisms. If an equivalent energy partition holds for Mt. Hood, the F_{ad} component of Eq. 1 would be 600 Wm^{-2}, a more speculative estimate than those given for the other components of the heat budget equation.

Inferred total heat discharge

On the basis of the preceding inferences and the planimetric area (9700 m^2) of the warm ground recorded on the infrared image of April 26, 1973, we estimate the heat loss via differential radiant exitance (F_b) to the atmosphere at approximately 1 MW.

The combined heat discharge via radiation (F_b), evaporation (F_e), conduction and diffusion (F_h) to the atmosphere, but exclusive of convective mass transfer and advective heat loss, is approximately 4 MW. Fumarolic mass transfer and advective heat loss (F_{ad}) may be of the order of 6 MW. The inferred total heat discharge is thus an order-of-magnitude estimate of 10 MW.

Geothermal flux of comparable volcanogenic hydrothermal systems

The geothermal flux has been reported to range from 20-50 Wm^{-2} for thermally active large Quaternary calderas in silicic to andesitic volcanic centers such as Torfajökull (Bödvarsson, 1961, p. 29-38) and Grimsvötn (Björnsson, 1974, p. 17), Iceland, and about 26 Wm^{-2} for six other caldera systems reviewed by Kovalev (1969, p. 15-16). The areas at these flux levels are the surface areas, above and approximately equivalent in area to the focus of subsurface heat generation, enclosed by near-vertical, volcano-tectonic bounding structures.

If we consider the Mt. Hood crater as the surface expression of such a volcano-tectonic unit, and as equivalent in area to the smallest circle containing all the major surface thermal anomalies (as mapped by infrared scanner), the area of the crater is about 225×10^3 m^2. The total heat flow at Mt. Hood, based on the above range in geothermal fluxes would fall between 4.5 and 11.4 MW. The average geothermal flux of Kovalev (1969) of 26 Wm^{-2} would yield 5.9 MW at Mt. Hood.

Heat flux at Mt. Hood

based on quasi-steady state heat flow,

volume of volcanic products, and age of volcanic edifice

The bulk of the energy yield from a volcanogenic hydrothermal system may be estimated from the volume of its volcanic products as a function of time. Mt. Hood's volume is 193 km^3 and it was built in late Pleistocene time on the site of Pliocene volcanic centers. If

the total volume of volcanic products over the last million years is 200 km^3, the average density of the cone is 2.4 g cm^{-3}, and the average heat content of volcanic products is 360 cal g^{-1} (1507 J g^{-1}), the average quasi-steady state heat flux has been 9.7 MW at Mt. Hood, an estimate comparable to those obtained by the preceding methods.

It is also possible to estimate the heat content of the dacite plug dome of Crater Rock. Since its volume is probably less than 1 km^3, its density somewhat greater than 2.4 g cm^{-2}, and its average heat content 1507 J g^{-1}, its total energy yield approached 4 x 10^{15}J. If dissipated over 220 years (or more) the heat flux attributable to the cooling of the plug dome would be less than .5 MW, clearly insufficient in itself to account for the heat flux emanating from the present fumarole fields.

Summary

Aerial infrared line-scan surveys flown in April 1972 and 1973 recorded the distribution of thermal areas associated with fumarole fields near the summit of Mt. Hood, between 3020 and 3230 m altitude and covering an area of 9700 m^2 in April 1973. The pattern of distribution of thermal areas suggests a generic relationship to peripheral structures and a brecciated zone that were controlled by or formed simultaneously with the extrusion of the Crater Rock hornblende-dacite plug dome, and a concentric fracture system associated with development of the present crater south of the summit. By analogy with similar thermal and fumarole fields of Mt. Baker and

Mt. St. Helens, the area of warm ground at Mt. Hood indicates the order of magnitude of the total heat discharge to be about 10 MW. This preliminary estimate is subject to revision when new thermal data from Mt. Hood become available.

Alternate methods for estimating the volcanogenic geothermal flux that assume a quasi-steady state heat flow also yield heat fluxes in the 5-11 MW range. Cooling of the dacite plug dome (Crater Rock) is judged to be insufficient to account for the heat flux at the fumarole field.

Acknowledgments

The authors gratefully acknowledge the cooperation extended by William S. Wise who made available to us his geologic field maps and annotated aerial photographs of the summit area of Mt. Hood and permitted us to use them in this report.

References cited

Ayres, F. D., and Cresswell, A. E., 1951, The Mount Hood fumaroles: Mazama, v. 33, no. 13, p. 33-40.

Birnie, R. W., 1973, Infrared radiation thermometry of Guatemalan volcanoes: Bull. Volcanologique, v. 37, no. 1, p. 1-36.

Bjornsson, Helgi, 1974, Explanation of Jökulhlaups from Grímsvötn, Vatnajökull, Iceland: Jökull, v. 24, p. 1-25.

Bodvarsson, Gunnar, 1961, Physical characteristics of natural heat resources in Iceland: Jökull, v. 11, p. 29-38.

Bowen, I. S., 1926, The ratio of heat losses by conduction and evaporation from any water surface: Physical Review, v. 27, p. 779-787.

Budyko, M. H., 1956, Teplovoi balans zemnoi poverkhnosti (The heat balance of the earth's surface): Hydrometeorological Press, Leningrad, 255 p. Translated by Nina A. Stepanova, U.S. Dept. of Commerce, Washington, D. C., 1958.

Crandell, D. R., and Meyer, Rubin, 1977, Late-glacial and postglacial eruptions at Mt. Hood, Oregon: Geol. Soc. America, Abstracts with Programs, v. 9, no. 4, p. 406.

Dawson, G. B., 1964, The nature and assessment of heat flow from hydrothermal areas: New Zealand Jour. Geol. and Geophysics, v. 7, no. 1, p. 155-171.

Friedman, J. D., and Frank, David, 1973, Aerial thermographic images of the Cascade Range, Washington, Oregon, and California: U.S. Geol. Survey Open-File Rept., (70 mm roll film), released Oct. 28, 1973.

Friedman, J. D., and Frank, David, 1977a, Thermal surveillance of active volcanoes using the Landsat-1 Data Collection System. Part 2: Infrared surveys, radiant flux and total heat discharge from Mount Baker volcano: U.S. Geol. Survey for NASA. Final report Landsat-1 experiment SR 251. Available from NTIS, Springfield, Va.

_____1977b, Thermal surveillance of active volcanoes using the Landsat-1 Data Collection System. Part 3: Heat discharge from Mount St. Helens, Washington. U.S. Geol. Survey for NASA. Final report Landsat-1 experiment SR 251. Available from NTIS, Springfield, Va.

Friedman, J. D., Preble, D. M., and Jakobsson, Sveinn, 1976, Geothermal flux through palagonitized tephra, Surtsey, Iceland--The Surtsey temperature-data-relay experiment via Landsat-1: U.S. Geol. Survey Jour. Research, v. 4, no. 6, p. 645-659.

Gouffe, Andre, 1945, Corrections d'ouverture des corps-noirs artificiels compte tenu des diffusions multiples internes: Rev. d'Optique Théorique et Instrumentale, v. 24, no. 1-3, p. 1-10.

Kienle, Jurgen, and Forbes, R. B., 1976, Augustine - evolution of a volcano: Ann. Rept. 1975-76, Geophysical Institute, Univ. of Alaska, p. 26-48.

Koide, H., and Bhattacharji, S., 1975, Formation of fractures around magmatic intrusions and their role in ore localization: Economic Geology, v. 70, no. 4, p. 781-799.

Kovalev, G. N., 1969, Teplovaya moshchnost' gidrotermal'nykh sistem; aktivnykh vulkanov (Heat output of hydrothermal systems and active volcanoes): Doklady of the Academy of Sciences USSR, Earth Science Sections, v. 186, p. 15-16.

Macdonald, Gordon, 1972, Volcanoes: Prentice-Hall, Inc., Englewood Cliffs, N. J., 510 p.

Perrey, A., 1865, Mémoires Acad. Dijon, II Sér. XIII, p. 240.

Phillips, K. N., and Collins, J. R., 1935, Fumaroles on Mount Hood: Mazama, v. 17, no. 12, p. 19-21.

Phillips, K. N., 1936, A chemical study of the fumaroles of Mount Hood: Mazama, v. 18, no. 12, p. 44-46.

Sapper, Karl, 1927, Vulkankunde: J. Engelhorns Nachf., Stuttgart, 424 p.

Sekioka, Mitsuru, and Yuhara, Kozo, 1974, Heat flux estimation in geothermal areas based on the heat balance of the ground surface: Jour. Geophys. Research, v. 79, no. 14, p. 2053-2058.

Sylvester, A. H., 1908, Is our noblest volcano awakening to new life?: National Geographic Mag., v. 19, no. 7, p. 515-525.

Wise, W. S., 1968, Geology of the Mt. Hood volcano: Andesite Conference guidebook: Internat. Upper Mantle Project Sci. Report 16-S and Oregon Dept. Geology and Mineral Industries Bull. 62, p. 81-98.

_____1969, Geology and petrology of the Mt. Hood area: A study of high Cascade volcanism: Geol. Soc. America Bull., v. 80, no. 6, p. 969-1006.

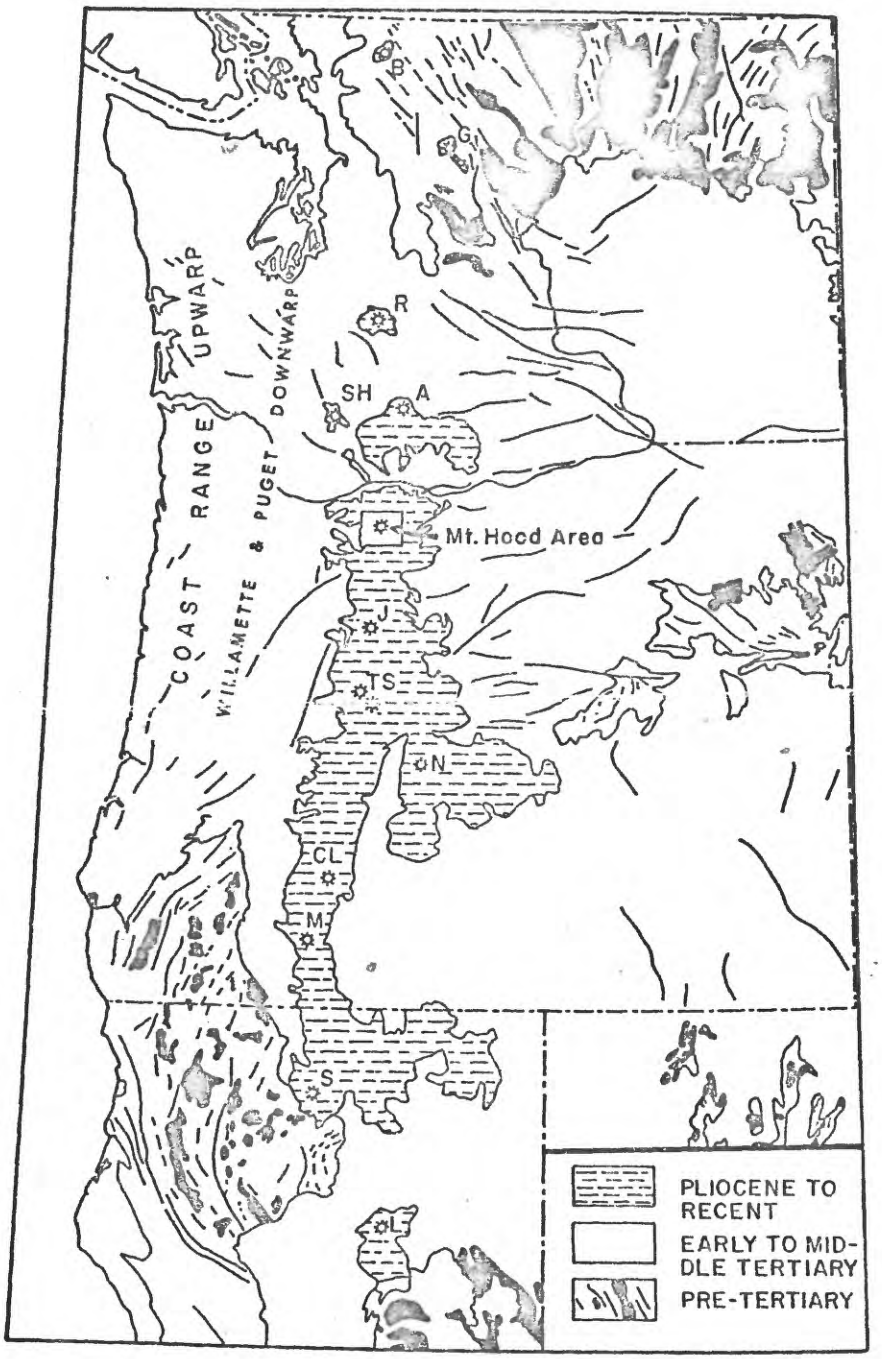

Figure 1: Tectonic index map of the Cascade Mountains. See caption.

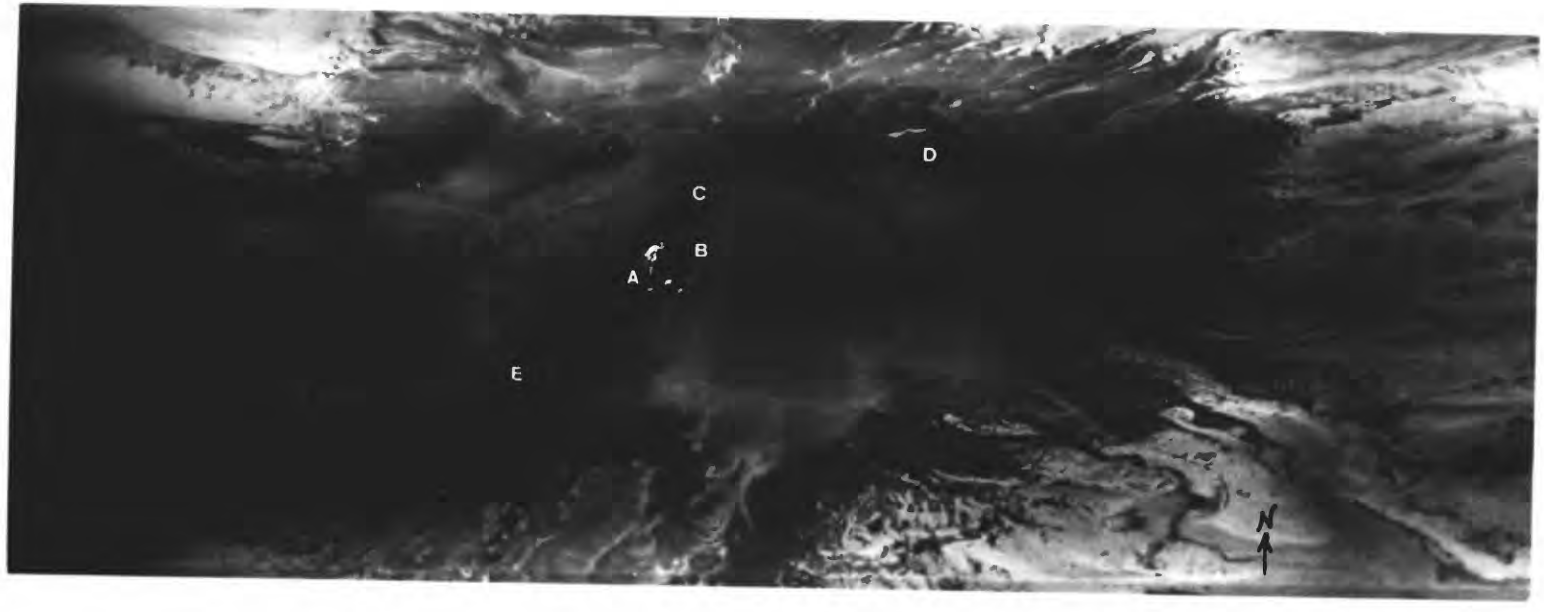

Figure 2: Infrared image of Mt. Hood. See caption.

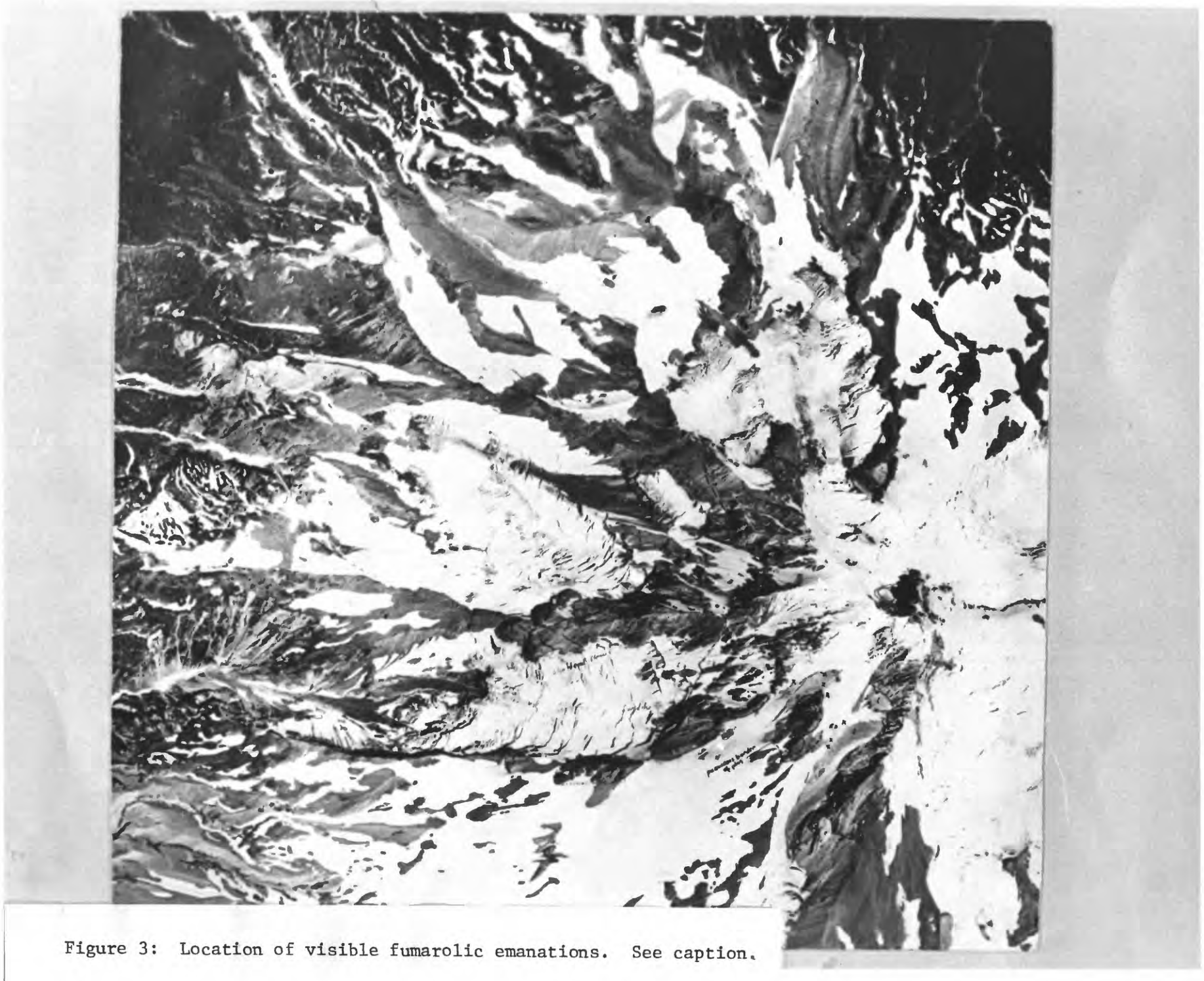

Figure 3: Location of visible fumarolic emanations. See caption.

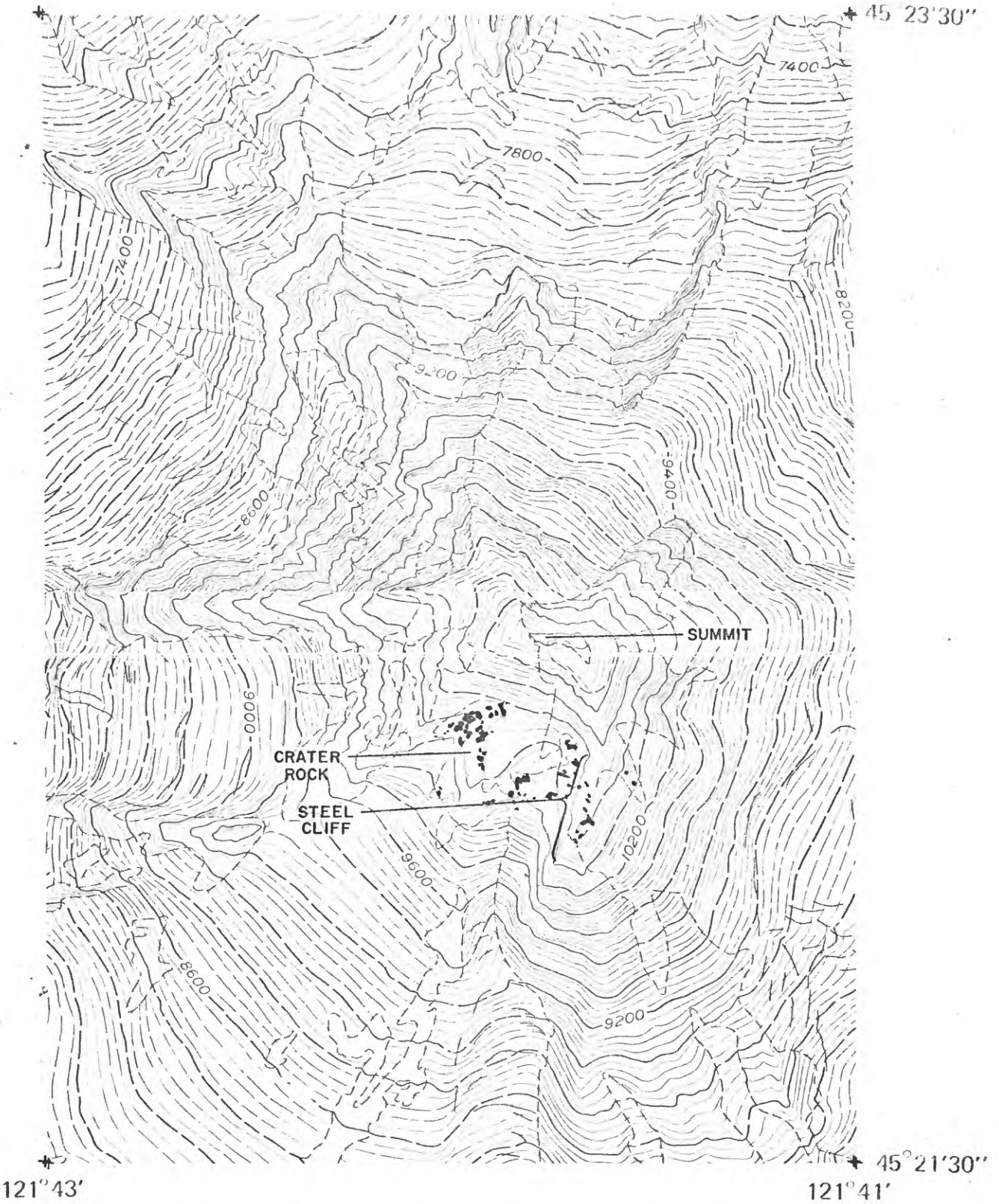

Base from U.S.G.S. 7.5' topo series
CATHEDRAL RIDGE, 1962,
MOUNT HOOD SOUTH, 1962,
OREGON

Figure 4: Topographic distribution of infrared anomalies of April 1973. See caption.

Figure 5: Infrared anomalies in relation to the Geology of the summit area of Mt. Hood, Oregon[1/]

Legend

Infrared anomalies where heat flux is 100 Wm^{-2} ±, associated with fumarole fields

no symbol — Glacier

Qt — Extensive talus slopes

Qm — Moraines, mostly associated with active glaciers

Qhh — Hornblende dacite debris fan with plug dome and breccia zone at Crater Rock.

Qhd — Reworked debris, postglacial, partly morainal, partly water-transported detritus

Qha — Mount Hood andesite flows

Qhp — Pyroclastic deposits interbedded with flows

U — Unmapped

1/ Based on infrared surveys of April 19, 1972, and geologic field mapping of William Wise between 1962 and 1965 at 1:24,000. Primary field maps were supplemented by a published small-scale map (Wise, 1968, p. 82-83).

Figure 5: INFRARED ANOMALIES OF 1973 IN RELATION TO GEOLOGY OF THE SUMMIT AREA OF MT HOOD OREGON . See caption.

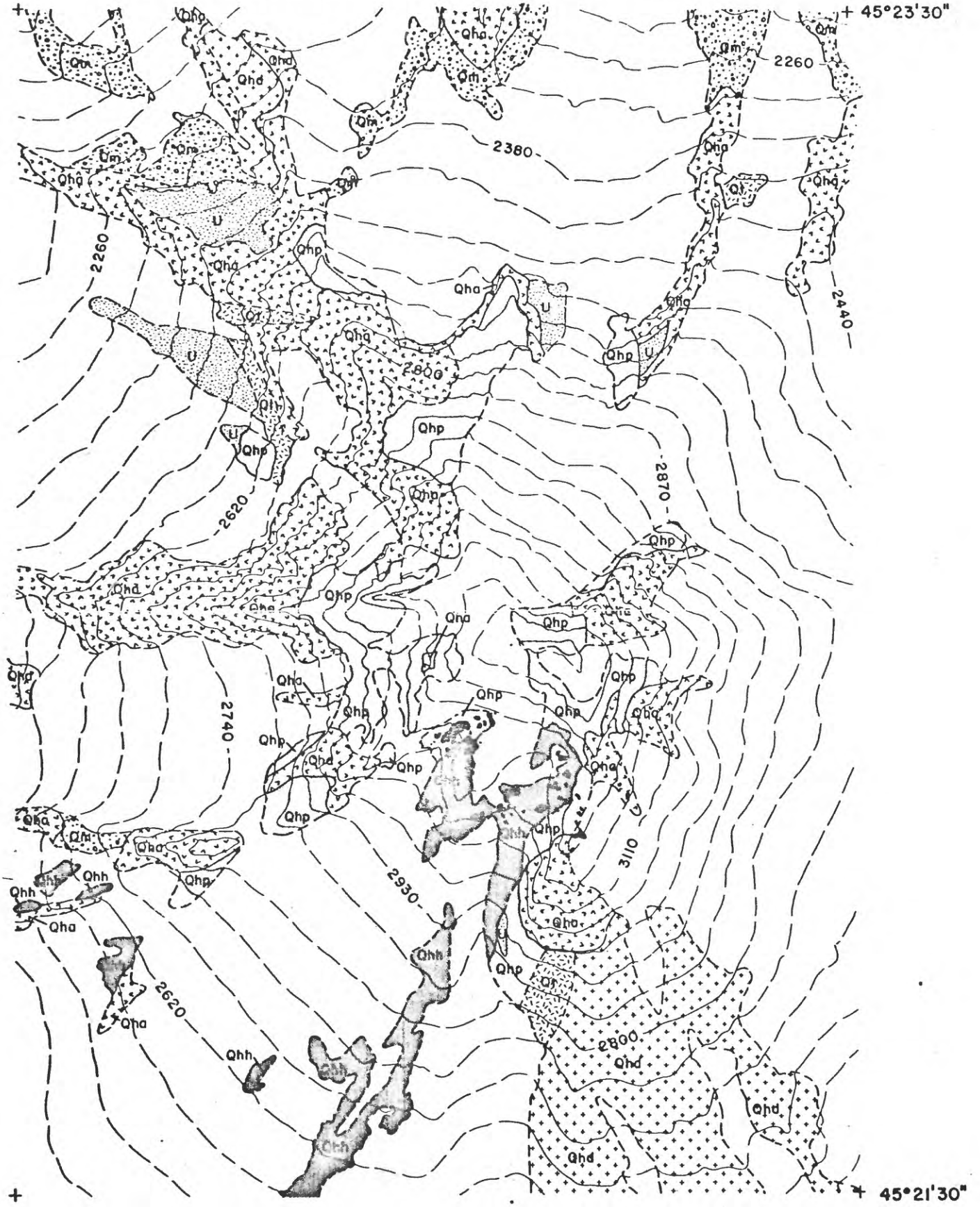

GEOLOGY MODIFIED FROM WISE, 1968

0 250 500 750 1000m

Base from U.S.G.S. 7.5' topo series
CATHEDRAL RIDGE, 1962,
MOUNT HOOD SOUTH, 1962,
OREGON

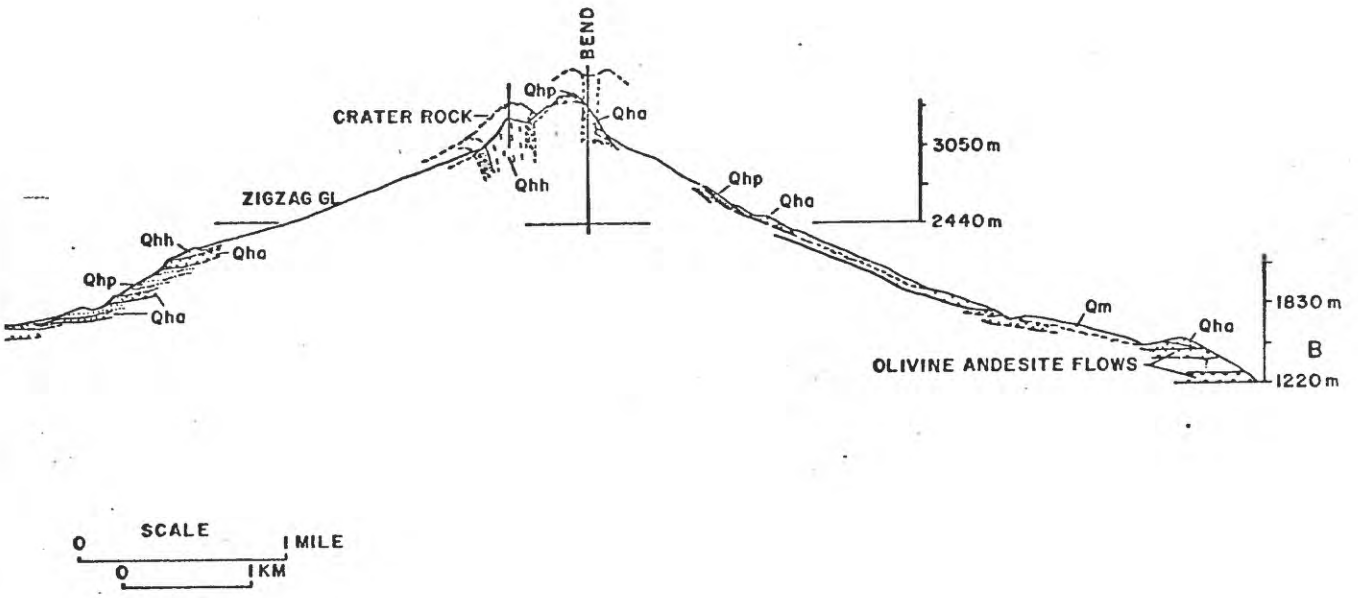

Figure 6: Structure section of Mt. Hood. See caption.